

## PREPARATION AND CHARACTERIZATION OF MAGNETIC COMPOSITES BASED ON A NATURAL ZEOLITE

MARLEN GUTIÉRREZ<sup>1,2</sup>, MAURICIO ESCUDEY<sup>1,2</sup>, JUAN ESCRIG<sup>1,2</sup>, JULIANO C. DENARDIN<sup>1,2</sup>, DORA ALTBIR<sup>1,2</sup>,  
JOSE D. FABRIS<sup>3</sup>, LUIS C. D. CAVALCANTE<sup>3</sup>, AND MARÍA TERESA GARCÍA-GONZÁLEZ<sup>4</sup>

<sup>1</sup> Universidad de Santiago de Chile, Av. B. O'Higgins 3363, 9170022 Santiago, Chile

<sup>2</sup> Center for the Development of Nanoscience and Nanotechnology, CEDENNA, 9170124, Santiago, Chile

<sup>3</sup> Departamento de Química, Universidade Federal de Minas Gerais, 31270-901 Belo Horizonte, Minas Gerais, Brazil

<sup>4</sup> Instituto de Ciencias Agrarias, Centro de Ciencias Medioambientales, Consejo Superior de Investigaciones Científicas, Calle Serrano 115, 28006 Madrid, Spain

**Abstract**—A magnetic composite was prepared by wet-impregnating a powder of a natural zeolite with a magnetic Fe oxide-containing synthetic material. Both starting materials were first characterized with X-ray diffraction, scanning electron microscopy, Mössbauer spectroscopy, and by isoelectric-point using vibrating-sample magnetometry. The synthetic Fe oxide-containing material was characterized as a mixture of magnetite (Fe<sub>3</sub>O<sub>4</sub>) and goethite ( $\alpha$ -FeOOH). From the <sup>57</sup>Fe Mössbauer analysis, the relative subspectral area for magnetite corresponds to 93(2)%; the remaining spectrum is assignable to goethite. After the impregnation process, magnetite was still identified in the composite material as a magnetic layer surrounding the zeolite particles; no magnetically ordered goethite could be detected. The Mössbauer pattern for this sample indicates a much more complex structure than for the precursor material, based on Fe oxides, with some more altered magnetite and an intense central doublet of (super)paramagnetic Fe<sup>3+</sup>, probably due to small Fe (hydr)oxides and/or to a residual contribution of Fe-bearing species from the starting zeolite material. The composite preparation procedure also promoted the change of the characteristic A-type zeolite to mordenite. The resulting magnetic composite presented a magnetic coercivity of as much as 0.140 A m<sup>-1</sup>, at 77 K. The final composite is now being evaluated as an adsorbent: results to date confirm that this novel magnetic material may have applications in the remediation of contaminated water bodies.

**Key Words**—Coercivity, Fe Oxide, Isoelectric Point, Magnetite, Magnetic Zeolite, Mössbauer Spectroscopy.

### INTRODUCTION

Zeolites are widespread in nature and are also relatively low-cost synthetic aluminosilicates, having a regular, nano-porous (pore sizes varying from 0.3 to 1 nm) crystallographic structure. They can behave as molecular sieves and are excellent cation exchangers due to their large specific surface area and negative structural surface charge, and have often been used to adsorb water contaminants, including heavy metals (Moirou *et al.*, 2000; Janotka *et al.*, 2003; Sprynskyy *et al.*, 2005; Motsi *et al.*, 2009; Calvo *et al.*, 2009). The crystal structure of zeolites significantly enhances their absorption capacity (Wang and Ariyanto, 2007; Zorpas *et al.*, 2008; Myroslav, 2009; Chutia *et al.*, 2009).

Magnetic carriers have been used in many applications, including biological-cells separation, wastewater treatment, and mineral-ore processing. Most environmental methods based on magnetic separation usually involve a discrete magnetic phase supported by non-magnetic particles, in order to increase their magnetic capability thereby making them more suitable for recovering

agglomerated solids from liquid media. After the impregnation process, magnetite was still identified in the composite material as a magnetic layer surrounding the zeolite particles (Bourlinos *et al.*, 2003; Schmauke *et al.*, 2003), either by surface precipitation of Fe oxides (Oliveira *et al.*, 2004), or, more specifically, by *in situ* combination of nano-particles of zeolite and magnetite (Fe<sub>3</sub>O<sub>4</sub>) (Shan *et al.*, 2006). Magnetic composites have the advantage of being easily separated from the liquid medium after use, *e.g.* with a simple permanent magnet, and they allow several cycles of cleaning, recovery, and reuse in environmental-remediation applications. The usefulness of such materials relies on the accurate control of their size, shape, heat of adsorption, and chemical characteristics (Xu *et al.*, 2007).

In the present work, a new method of preparing magnetic, aluminosilicate-based composites, by combining a natural zeolite with a synthetic magnetic Fe oxide, is proposed. The resulting material is described and characterized.

### MATERIALS AND METHODS

The sample containing the natural zeolite, collected from a mine located at 36°16'S 71°40'W (Parral, Chile), was ground to pass a 2 mm sieve (Retsch, Haan,

\* E-mail address of corresponding author:

mauricio.escudey@usach.cl

DOI: 10.1346/CCMN.2010.0580501

Germany). The natural zeolite was characterized later as type-A zeolite. The  $<2\ \mu\text{m}$  size particles were separated by the Jackson (1969) sedimentation procedure. To prepare the synthetic magnetic Fe oxide, 0.250 g of  $\text{FeSO}_4$  was dissolved in 20.0 mL of double distilled water at 363 K previously degassed with  $\text{N}_2$ . After complete dissolution, 0.033 g of  $\text{KNO}_3$  was added and then 0.5 mL of concentrated ammonia was dropped into the solution, to precipitate the Fe oxides. To prepare the magnetic zeolite, the wet impregnation method in excess solvent was used, in accordance with a procedure described by Gil-Llambias and Escudéy-Castro (1982) and Escudéy and Gil-Llambias (1985). The synthesis involves a similar procedure to that used to prepare the magnetic Fe oxide. Briefly, after the dissolution of 0.250 g of  $\text{FeSO}_4$ , 0.250 g of natural zeolite was added, followed by the addition of 0.033 g of  $\text{KNO}_3$  and 0.5 mL of concentrated ammonia.

The starting natural zeolite, the synthetic Fe oxide, and the zeolite-based magnetic composite samples were

characterized by means of X-ray diffraction (XRD), scanning electron microscopy (SEM), micro-electrophoresis,  $^{57}\text{Fe}$  Mössbauer spectroscopy, and vibrating sample magnetometry.

The mineralogy of the samples was identified by comparing powder XRD patterns obtained for randomly oriented powder mounts, using a Philips X'Pert diffractometer (graphite-monochromated  $\text{CuK}\alpha$  radiation) with data from the International Center for Diffraction Data-Powder Diffraction File (ICDD-PDF).

The grain morphology of the powder samples was analyzed using a Zeiss DSM 960 scanning electron microscope equipped with a backscattered electron detector. The samples were oven dried at  $50^\circ\text{C}$ , deposited on carbon grids, and coated with carbon prior to examination.

The room-temperature  $^{57}\text{Fe}$  Mössbauer analysis was performed using a constant-acceleration transmission spectrometer and a  $^{57}\text{Co}/\text{Rh}$  source.

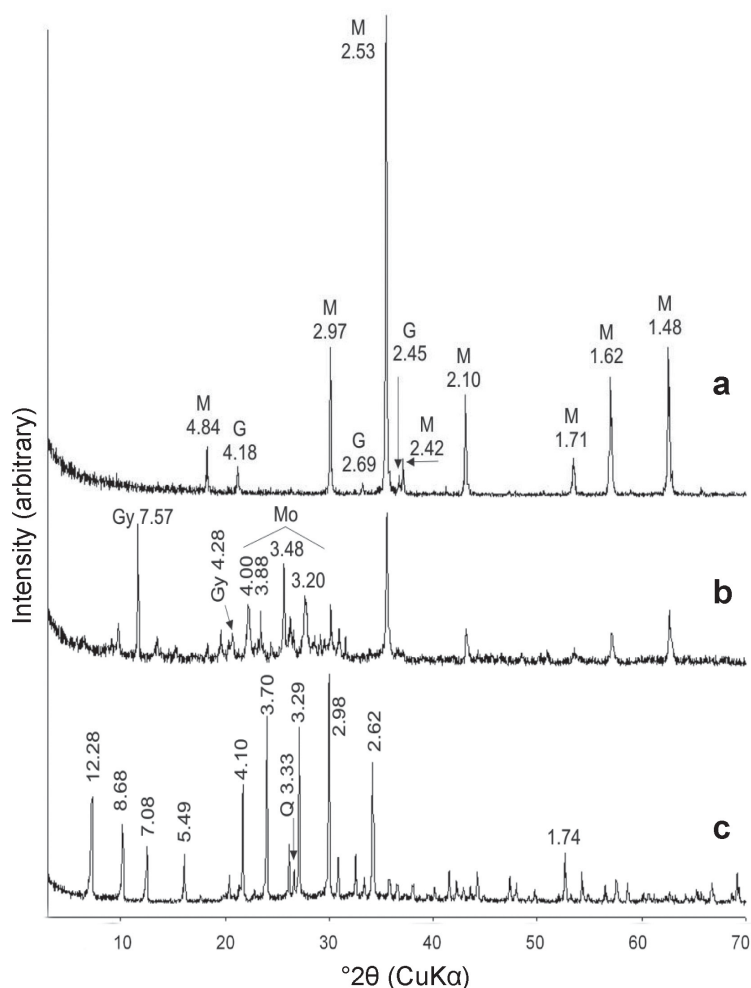


Figure 1. XRD patterns of (a) synthetic Fe oxide, (b) magnetic zeolite, and (c) natural zeolite. The numbers indicate the  $d$  values ( $\times 10^{-1}\ \text{nm}$ ) of the main peaks.

The isoelectric point (IEP) was determined using the micro-electrophoresis method. The electrophoretic mobilities (EM) were measured with a zeta-meter (ZM-77) apparatus. Dilute suspensions (containing  $\sim 0.05 \text{ g L}^{-1}$ ) were prepared in  $10^{-3} \text{ mol L}^{-1}$  KCl. The pH was adjusted with  $10^{-2} \text{ mol L}^{-1}$  HCl or NaOH. The EM were averaged and the zeta potential (ZP) was calculated using the Helmholtz-Smoluchowski equation (Hunter, 1981). The IEP was determined as the pH value at ZP = 0.

The magnetic measurements were made with a vibrating sample magnetometer (VSM). Sample magnetization was determined as a function of an external applied field (hysteresis curve) at room temperature and at 77 K.

## RESULTS AND DISCUSSIONS

The XRD data for the synthetic Fe oxide (Figure 1a) revealed the co-existence of magnetite (M) (reflections at 4.84, 2.97, 2.53, 2.42, 2.10, 1.71, 1.62, and 1.48 Å, ICDD-PDF card # 01-085-1436) and goethite (G) (reflections at 4.18, 2.69, and 2.45 Å, ICDD-PDF card # 00-029-0713), of which magnetite was the more abundant. The sub-micromorphological study (Figure 2a) showed sphere-like to truncated octahedral crystals of magnetite and acicular crystals of goethite.

In the case of the natural zeolite (Figure 1c), all diffraction maxima were characteristic of an A-type zeolite (ICDD-PDF card # 01-076-1508). Only a small proportion of quartz (Q) (3.33 Å) was detected. The SEM images (Figure 2b) indicate an homogeneous, porous specimen.

The XRD pattern for the magnetic zeolite (Figure 1b) indicates the occurrence of mordenite (Mo) (reflections at 4.00, 3.88, 3.48, and 3.20 Å; ICDD-PDF card # 00-006-0239) together with a considerable proportion of magnetite (M) (4.84, 2.97, 2.53, 2.10, 1.62, and 1.48 Å) and traces of gypsum (Gy) (7.57, 4.28, and 3.07 Å, ICDD-PDF card # 00-036-0432). From the SEM images (Figure 2c), only sphere-like crystals, character-

istic of magnetite, were observed. After the impregnation procedure,  $\text{Ca}^{2+}$  was found to be released from the natural zeolite, changing its original A-type structure to that of mordenite. Magnetite appears to achieve a greater degree of crystallinity than goethite.  $\text{Ca}^{2+}$  reacts with  $\text{SO}_4^{2-}$  ions of the Fe-source solution, used in the preparation of the composite, to form traces of gypsum ( $\text{CaSO}_4 \cdot 2\text{H}_2\text{O}$ ) on the surfaces of mordenite grains.

Fitted Mössbauer parameters of the spectra in Figures 3a and 3b are presented in Table 1. The spectrum for the synthetic Fe oxides (Figure 3a) shows a typical hyperfine pattern (relative subspectral area,  $AR = 93(2)$ ) of magnetite, with two magnetically split sextets, one with an isomer shift relative to  $\alpha\text{Fe}$  ( $\delta = 0.333(7) \text{ mm s}^{-1}$ , magnetic hyperfine field,  $B_{\text{hf}} = 49.01(5) \text{ tesla}$ , which is assignable to  $\text{Fe}^{3+}$  in tetrahedral sites ( $A$ , in Table 1)), and the other with  $\delta = 0.645(5) \text{ mm s}^{-1}$ ,  $B_{\text{hf}} = 45.51(4) \text{ tesla}$ , due to mixed valence  $\text{Fe}^{3+}/\text{Fe}^{2+}$  in octahedral sites ( $B$ , in Table 1) of the spinel structure. Consistent with XRD and SEM results, small amounts of goethite ( $\alpha\text{-FeOOH}$ ,  $AR = 7(2)$ ; Table 1) occur also. For the zeolite-based magnetic composite, magnetite is still visible in the Mössbauer spectrum (Figure 3b) even though some alteration seems to have taken place, probably involving  $\text{Fe}^{2+} \rightarrow \text{Fe}^{3+}$  oxidation in octahedral sites, and somehow releasing  $\text{Fe}^{3+}$  to the grain surface to form (super)-paramagnetic Fe (hydr)oxides species in very small (presumably not much greater than a few tens of nm across) particles. Some of the  $\text{Fe}^{3+}$  contribution to the spectrum of the zeolite-based magnetic composite may also be due to ferric species of the natural zeolite sample, as indicated by the central doublet appearing in the experimental spectrum of Figure 3c.

The ZP vs. pH curves for natural zeolite, synthetic Fe oxides (magnetite-goethite mixture), and magnetic composite samples are shown in Figure 4. The natural zeolite presents a small IEP value (2.3) and constant negative surface charge over a wide pH range. The synthetic Fe-oxides sample presents a pH-dependent variable surface charge (IEP = 6.5), which is characteristic of

Table 1. 298 K-Mössbauer parameters for synthetic Fe oxide-containing material and zeolite-based magnetic composite.

Sample	Assignment	$\Delta$ (mm s <sup>-1</sup> )	$\epsilon$ ( $\Delta/\text{mm s}^{-1}$ )	$\Gamma$ (mm s <sup>-1</sup> )	$B_{\text{hf}}$ (T)	$AR$ (%)
Fe oxide	Mt- $A$	0.333(7)	0.01(1)	0.41(2)	49.01(5)	40(2)
	Mt- $B$	0.645(5)	-0.001(1)	0.43(2)	45.51(4)	53(2)
	$\alpha\text{-FeOOH}$	0.32(4)	-0.27(8)	0.4(1)	37.0(3)	7(2)
Magnetic zeolite	Mt- $A$	0.330(4)	-0.020(8)	0.51(2)	48.39(3)	37(1)
	Mt- $B$	0.618(9)	-0.07(2)	0.79(3)	44.80(7)	35(2)
	$\text{Fe}^{3+}$	0.360(4)	0.718(7)	0.58(1)		28.0(3)

$\delta$  = isomer shift relative to  $\alpha\text{Fe}$ ;  $\epsilon$  = quadrupole shift;  $\Delta$  = quadrupole splitting;  $\Gamma$  = line width;  $B_{\text{hf}}$  = magnetic hyperfine field;  $AR$  = relative subspectral area. Mt = magnetite;  $\alpha\text{-FeOOH}$  = goethite.  $A$  and  $B$  denote tetrahedral and octahedral coordination sites of the spinel structure of magnetite. The numbers in parentheses are uncertainties over the last significant digit, as estimated from the least-squares fitting algorithm.

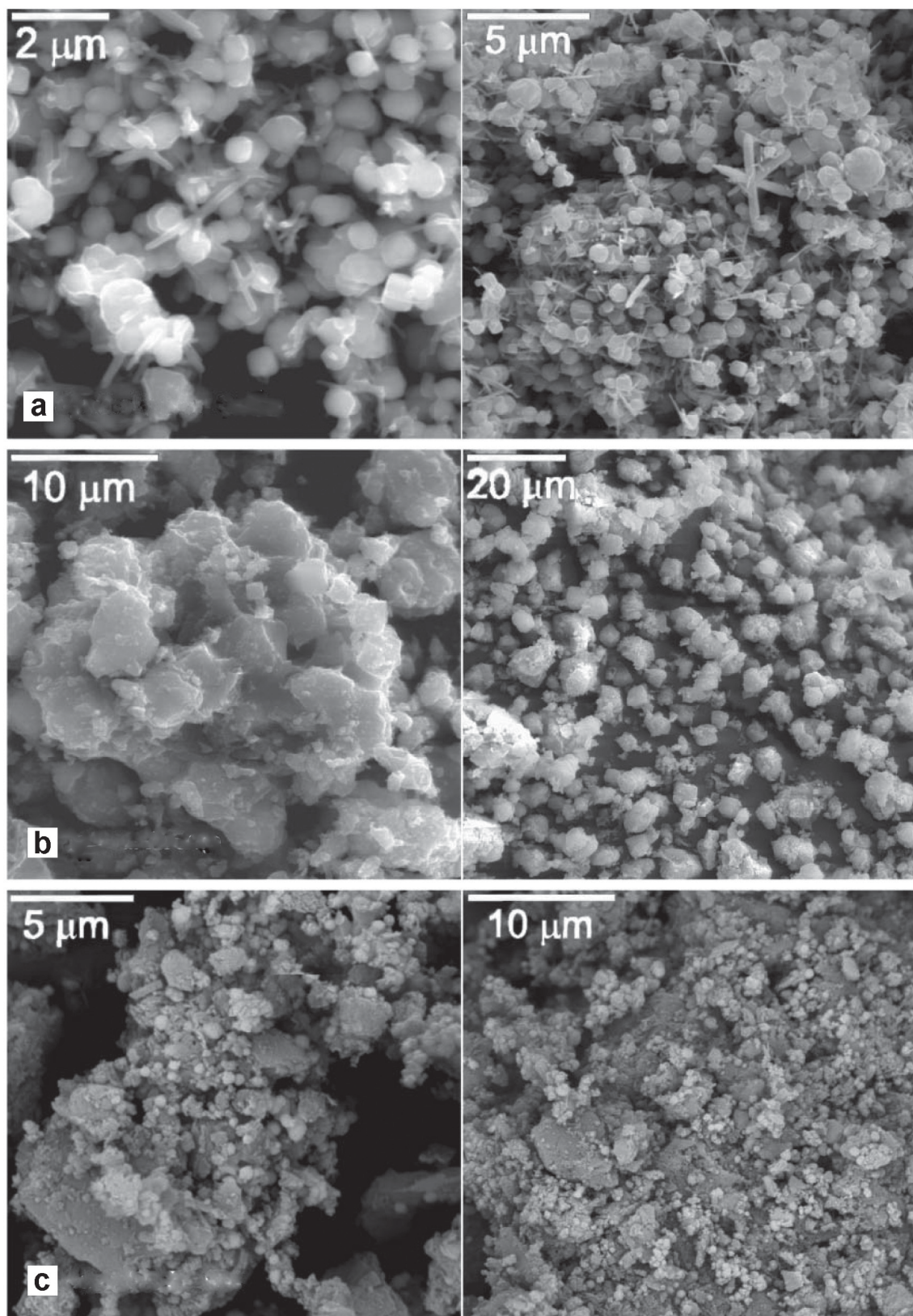


Figure 2. SEM images of (a) synthetic Fe oxide, (b) natural zeolite, and (c) magnetic zeolite.

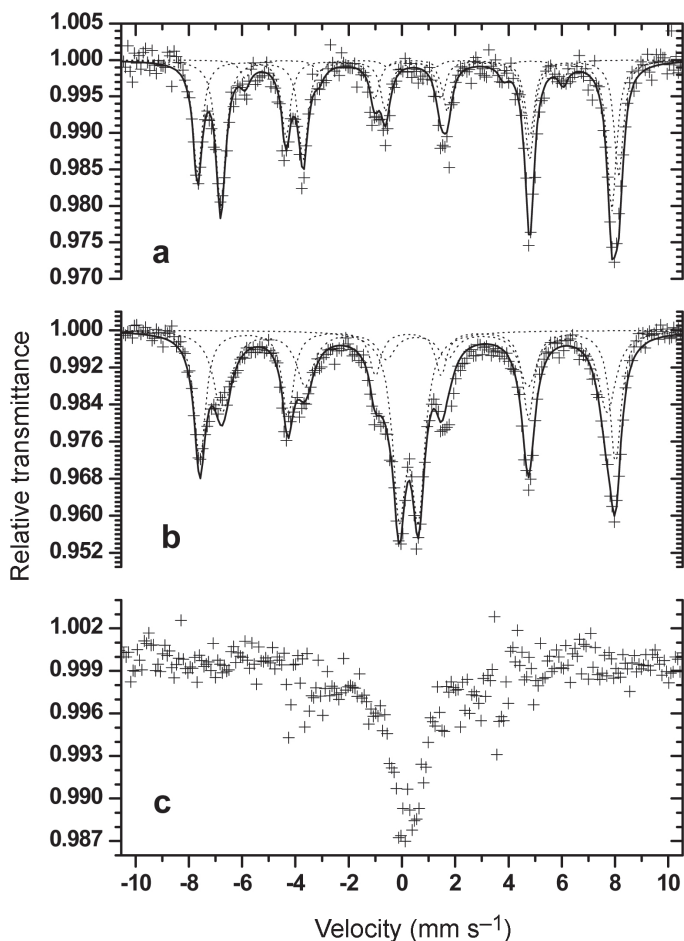


Figure 3. Room-temperature Mössbauer spectra for (a) synthetic Fe oxide, (b) magnetic zeolite, and (c) natural zeolite.

these kinds of materials (Parks, 1969). The reported IEP values for the binary composite are usually equivalent to the average of the IEP values of the starting materials (Gil-Llambias and Escudey-Castro, 1982; Escudey and

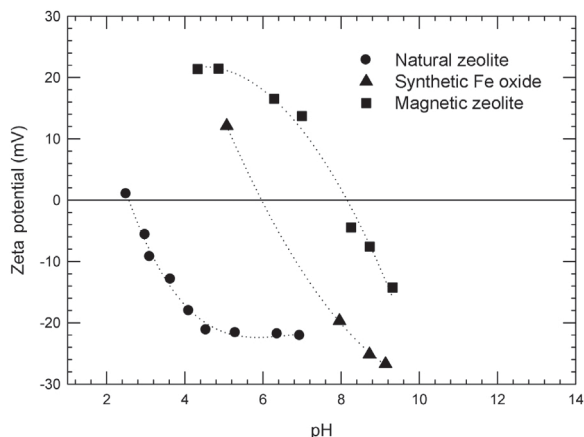


Figure 4. Zeta potential vs. pH curves for synthetic Fe oxide, natural zeolite, and magnetic zeolite.

Gil-Llambias, 1985; Parks, 1969). For the present magnetic zeolite-based composite, however, the IEP value is 8.2, greater than that of its individual constituents. This apparent inconsistency can be explained by taking into account the changes in mineralogy and external surface composition, with resultant impact on the surface charge and on the SEM and XRD results, of the particles. Zeta-potential measurements are very sensitive to the composition of the external surface (Gil-Llambias and Escudey-Castro, 1982; Parks, 1969). Mineralogical modifications of the zeolite and Fe oxides and the occurrence of gypsum on the composite surface probably account for the greater IEP value observed for this magnetic composite (Escudey and Gil-Llambias, 1985).

The pH-dependent surface charge found for the magnetic composite favors the adsorption of cations and anions from an electrostatic standpoint, by controlling the pH conditions of the medium, thereby increasing its potential applications in environmental remediation.

The VSM hysteresis curve is the fingerprint criterion to identify and characterize magnetic materials and gives

important information about their magnetic characteristics such as coercivity (the reverse magnetic field needed to zero the magnetization), remanence (the residual magnetization at zero-field under reversal of applied field), and saturation magnetization.

The saturation magnetization established for these synthetic Fe oxides (magnetite-goethite mixture) is  $78 \text{ A m}^2 \text{ kg}^{-1}$ , which is somewhat smaller, as expected, than that of a pure magnetite ( $92 \text{ A m}^2 \text{ kg}^{-1}$ ) (Buschow, 2006). The magnetization curve for this natural zeolite indicates that no magnetic component was present on the material before impregnation with the Fe oxides (Figure 5). However, after impregnation, a magnetite layer was formed on the surfaces of the grains and the saturation magnetization increased to  $11 \text{ A m}^2 \text{ kg}^{-1}$  (Figure 5). In spite of being  $\sim 14\%$  of the value obtained for the synthetic Fe oxide sample, it was large enough to be considered as a magnetic composite, and this is consistent with the proportion of Fe oxides used in the preparation. The hysteresis loops for the Fe oxides (curve not shown) and zeolite-based magnetic composite samples (Figure 5) are typical of fine, mono-domain particles containing magnetically ordered phases.

The coercivity of both the magnetic Fe oxide and zeolites impregnated with magnetite was  $70 \times 10^{-3} \text{ A m}^{-1}$ , at 298 K, but increased to  $140 \times 10^{-3} \text{ A m}^{-1}$ , at 77 K. Increasing the coercivity field value at lower temperature is consistent with commonly observed behavior in fine, superparamagnetic particles. The paramagnetic relaxation process for some of these nano-particles is probably blocked at 77 K, contributing to an increase in both coercivity and remanence.

For the Fe oxides and the magnetic composite, the saturation magnetization remained constant over a 12-week aging period of the material in air, indicating quite a good magnetic stability.

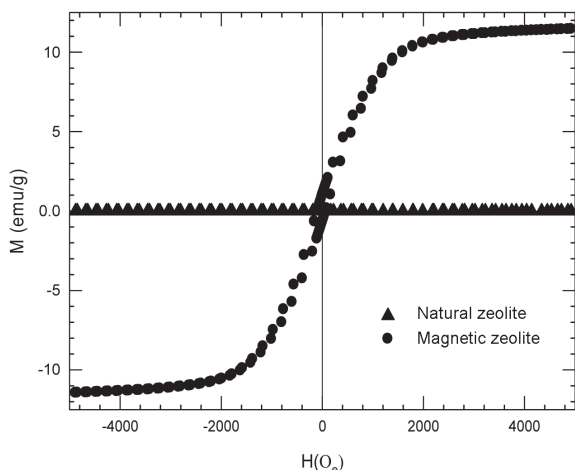


Figure 5. Hysteresis loops of natural zeolite and the synthesized magnetic zeolite.

The magnetic composite is currently being evaluated as a potential adsorbent. Preliminary results, from systematic tests now in progress, have confirmed that this novel material is potentially viable as an alternative for environmental cleaning of contaminated water bodies.

## CONCLUSIONS

The wet impregnation method proposed in this work allows the preparation of a zeolite-based magnetic composite. The impregnation procedure induces the magnetite to be crystallized on the surface of the zeolite. The composite presents a pH-dependent surface charge which is useful for adsorption of cations or anions, depending on the environmental conditions, in the case of remediation applications. The hysteresis loops for the magnetic composite show typical hysteresis curves of fine particles containing mono-domain, magnetically ordered phases, increasing the coercive field and remanence at low temperature, indicating at least partial blocking of the superparamagnetic relaxation process. Preliminary experimental tests at a laboratory scale confirm the possible viability of this novel material in the environmental remediation of contaminated water bodies.

## ACKNOWLEDGMENTS

This work was partially supported by FONDECYT under projects 1070116, 11070010, 1080164, and 1080300, Millennium Science Nucleus Basic and Applied Magnetism No. P06-022F, Financiamiento Basal para Centros Científicos y Tecnológicos de Excelencia No. FB0807, Prosul-CNPq (Brazil; grant 490132/2006-5), FAPEMIG (Brazil), AFOSR (Award No FA9550-07-1-0040), and Spanish Ministry of Science and Innovation (AGL 2005-07017-C03-03). M. Gutiérrez acknowledges a scholarship from CONICYT (Chile).

## REFERENCES

- Bourlinos, A.B., Zboril, R., and Petridis, D. (2003) A simple route towards magnetically modified zeolites. *Microporous and Mesoporous Materials*, **58**, 155–162.
- Buschow, K.H.J. (2006) *Handbook of Magnetic Material*. Elsevier, Amsterdam, **16**, p. 450.
- Calvo, B., Canoira, L., Morante, F., Martinez-Bedia, J.M., Vinagre, C., Garcia-Gonzalez, J.E., Elsen, J., and Alcantara, R. (2009) Continuous elimination of  $\text{Pb}^{2+}$ ,  $\text{Cu}^{2+}$ ,  $\text{Zn}^{2+}$ ,  $\text{H}^+$  and  $\text{NH}_4^+$  from acidic waters by ionic exchange on natural zeolites. *Journal of Hazardous Materials*, **166**, 619–627.
- Chutia, P., Kato, S., Kojima, T., and Satokama, S. (2009) Adsorption of As (V) on surfactant-modified natural zeolites. *Journal of Hazardous Materials*, **162**, 204–211.
- Escudey, M. and Gil-Llambias, F. (1985) Effect of cation and anion adsorption on the electrophoretic behavior of  $\text{MoO}_3/\gamma\text{-Al}_2\text{O}_3$  catalysts. *Journal of Colloid and Interface Science*, **107**, 272–275.
- Gil-Llambias, F.J. and Escudey-Castro, A.M. (1982) Use of zero point charge measurements in determining the apparent surface coverage of molybdenum in  $\text{MoO}_3/\gamma\text{-Al}_2\text{O}_3$  catalysts. *Journal of the Chemical Society, Chemical Communications*, **9**, 478–479.
- Hunter, R.J. (1981) *Zeta Potential in Colloid Science*:

- Principles and Applications*. Academic Press, London.
- Jackson, M.L. (1969) *Soil Chemical Analysis: Advanced Course*, 3<sup>rd</sup> edition. Published by the author, Madison, Wisconsin, USA, p. 894.
- Janotka, I., Krajčí, L., and Dzivák, M. (2003) Properties and utilization of zeolite-blended portland cements. *Clays and Clay Minerals*, **51**, 616–624.
- Moirou, A., Vaxevanidou, A., Christidis, G.E., and Paspaliaris I. (2000) Ion exchange of zeolite Na-Pc with  $Pb^{2+}$ ,  $Zn^{2+}$ , and  $Ni^{2+}$  ions. *Clays and Clay Minerals*, **48**, 563–571.
- Motsi, T., Rowson, N.A., and Simmons, M.J.H (2009) Adsorption of heavy metals from acid mine drainage by natural zeolite. *International Journal of Mineral Processing*, **92**, 42–48.
- Myroslav, S. (2009) Solid-liquid-solid extraction of heavy metals (Cr, Cu, Cd, Ni and Pb) in aqueous systems of zeolite-sewage sludge. *Journal of Hazardous Materials*, **161**, 1377–1383.
- Oliveira, L.C.A., Petkowicz, D.I., Smaniotto, A., and Pergher, S.B.C. (2004) Magnetic zeolites: a new adsorbent for removal of metallic contaminants from water. *Water Research*, **38**, 3699–3704.
- Parks, G.A. (1969) Aqueous surface chemistry of oxides and complex oxide minerals. Pp. 121–160 in: *Equilibrium Concepts in Natural Water Systems* (R.F. Gould, editor). Advances in Chemistry Series No. **67**, American Chemical Society, Washington D.C.
- Schmauke, T., Menzel, M., and Roduner, E. (2003) Magnetic properties and oxidation state of iron in bimetallic PtFe/KL zeolite catalysts. *Journal of Molecular Catalysis A: Chemistry*, **194**, 211–225.
- Shan, W., Yu, T., Wang, B., Hu, J.K., Zhan, Y.H., Wang, X.Y., and Tang, Y. (2006) Magnetically separable nanozeolites: promising candidates for bio-applications. *Chemistry of Materials*, **18**, 3169–3172.
- Sprynskyy, M., Lebedynets, M., Terzyk, A.P., Kowalczyk, P., Namieśnik, J., and Buszewski, B. (2005) Ammonium sorption from aqueous solutions by the natural zeolite Transcarpathian clinoptilolite studied under dynamic conditions. *Journal of Colloid and Interface Science*, **284**, 408–415.
- Wang, S. and Ariyanto, E. (2007) Competitive adsorption of malachite green and Pb ions on natural zeolite. *Journal of Colloid and Interface Science*, **314**, 25–31.
- Xu, R., Pang, W., Yu, J., Huo, Q., and Chen, J. (2007) *Chemistry of Zeolite and related Porous Materials. Synthesis and Structure*. Wiley, New York.
- Zorpas, A.A., Inglezakis, V.J., and Loizidou, M. (2008) Heavy metals fractionation before, during and after composting of sewage sludge with natural zeolite. *Waste Management*, **2**, 2054–2060.

(Received 6 April 2009; revised 23 July 2010; Ms. 304; A.E. H. Stanjek)